

Crossover from two-dimensional to three-dimensional superconducting states in bismuth-based cuprate superconductor

Jing Guo^{1,6}, Yazhou Zhou^{1,6}, Cheng Huang^{1,2,6}, Shu Cai¹, Yutao Sheng^{1,2}, Genda Gu³, Chongli Yang¹, Gongchang Lin^{1,2}, Ke Yang⁴, Aiguo Li⁴, Qi Wu¹, Tao Xiang^{1,2,5} and Liling Sun^{1,2,5*}

To decipher the mechanism of high-temperature superconductivity, it is important to know how the superconducting pairing emerges from the unusual normal states of cuprate superconductors^{1–4}, including the pseudogap^{5,6}, strange metal^{7,8} and anomalous Fermi liquid⁹ phases. A long-standing issue is how the superconducting pairing is formed and condensed in the strange metal phase, because this is where the superconducting transition temperature is highest. Here, we use state-of-the-art high-pressure measurements to report the experimental observation of a pressure-induced crossover from two- to three-dimensional (2D to 3D) superconducting states in optimally doped Bi₂Sr₂CaCu₂O_{8+δ} bulk superconductor. By analysing the temperature dependence of the resistance, we find that the 2D superconducting transition exhibits a Berezinskii-Kosterlitz-Thouless-like behaviour¹⁰. The emergence of this 2D superconducting transition provides direct evidence that the strange metal state is predominantly 2D-like. This is important for a thorough understanding of the phase diagram of cuprate superconductors.

Since the discovery of superconductivity in the Ba-doped cuprate La₂CuO₄ in 1986¹¹, more than two hundred cuprate superconductors, grouped into seven families with two fashions of hole and electron doping, have been found^{12–14}. Structurally, the hole-doped cuprate superconductors have a peculiar octagonal or pyramid lattice with apical oxygen, which intrinsically leads to a more complicated lattice that is unsteady upon cooling due to the Jahn–Teller effect. Therefore, their normal states at temperatures above those where superconductivity occurs, such as the pseudogap^{5,6}, strange metal^{7,8} and anomalous Fermi liquid^{2,9} states, are full of the unknown physics determining superconductivity^{1–3}. Although a lot of theoretical progress has been made regarding the superconducting mechanism of these high transition temperature (high- T_c) superconductors^{4,15–19}, a unified understanding of how the superconducting state connects with these unusual normal states is still lacking²⁰.

Because the strange metal state of the optimally doped superconductor not only can develop the superconducting state with the highest T_c but also links the pseudogap and the anomalous Fermi liquid states, it is of great interest to take the strange metal state as a breakthrough point to reveal the underlying physics of cuprate superconductors. In this high-pressure study, we chose to investigate the optimally doped Bi₂Sr₂CaCu₂O_{8+δ} (Bi-2212) single crystal, a typical nearly two-dimensional (2D) high- T_c superconductor with the

strange metal normal state, which has been widely studied in recent years^{5,6,14,21–25}. We performed in situ high-pressure measurements of the resistance, magnetoresistance and alternating current (a.c.) susceptibility of the samples, in an attempt to reveal the connection between the strange metal state and the superconducting state.

Figure 1a presents plots of temperature (T) versus in-plane resistance (R_{ab}) for one of the high-quality Bi-2212 samples while subjected to pressures ranging from 0.97 GPa to 13.7 GPa. When measured at 0.97 GPa, $R_{ab}(T)$ displays a T -linear behaviour over a broad temperature range above its onset T_c at ~96 K, showing that the sample is nearly in the ambient-pressure strange metal normal state of the optimally doped superconductor^{7,8}. At a pressure of 2.8 GPa, we found a small resistance drop at a temperature ~20 K higher than its ambient-pressure T_c . This higher-temperature drop becomes more visible at 5 GPa and pronounced on further compression. To characterize the higher-temperature resistance drop emerging from the strange metal state, we applied the magnetic field perpendicular to the a - b plane for the sample subjected to 9 GPa, and found that the drop is continuously suppressed by the magnetic field until it vanishes at 1 T (Fig. 1b). To confirm this pressure-induced ‘two-step drop behaviour’, we repeated the measurements with new samples for five independent runs, and proved that the results were reproducible. Figure 1c shows the results obtained from one of the experimental runs, which demonstrates that the higher-temperature resistance drop appears at 2.9 GPa and prevails up to 10.2 GPa, the maximum pressure of this run. On application of the perpendicular magnetic field to the compressed sample at 10.2 GPa, similar behaviour was observed, with the higher-temperature resistance drop shifting to a lower temperature on increasing the magnetic field and disappearing at 1 T (Fig. 1d). These results indicate that the higher-temperature drop is associated with a superconducting transition.

To further identify the differences between these two superconducting states, we concurrently performed in situ high-pressure measurements of the in-plane resistance (R_{ab}) and out-plane resistance (R_c) of the sample, with the same setup. As shown in Fig. 2a–d, the $R_c(T)$ of the sample when subjected to pressures from 6.0 GPa to 9.0 GPa shows a non-metallic feature before the superconducting transition, while $R_{ab}(T)$ displays metallic behaviour with a T -linear characteristic. Looking in detail at $R_c(T)$, we find a kink-like feature at 116 K (Fig. 2a) in the monotonically increasing $R_c(T)$ on cooling, until an abrupt drop appears at 90 K (6 GPa). The lower-temperature

¹Institute of Physics, National Laboratory for Condensed Matter Physics, Chinese Academy of Sciences, Beijing, China. ²University of Chinese Academy of Sciences, Beijing, China. ³Condensed Matter Physics & Materials Science Department, Brookhaven National Laboratory, Upton, NY, USA. ⁴Shanghai Synchrotron Radiation Facilities, Shanghai, China. ⁵Songshan Lake Materials Laboratory, Dongguan, Guangdong, China. ⁶These authors contributed equally: Jing Guo, Yazhou Zhou, Cheng Huang. *e-mail: llsun@iphy.ac.cn

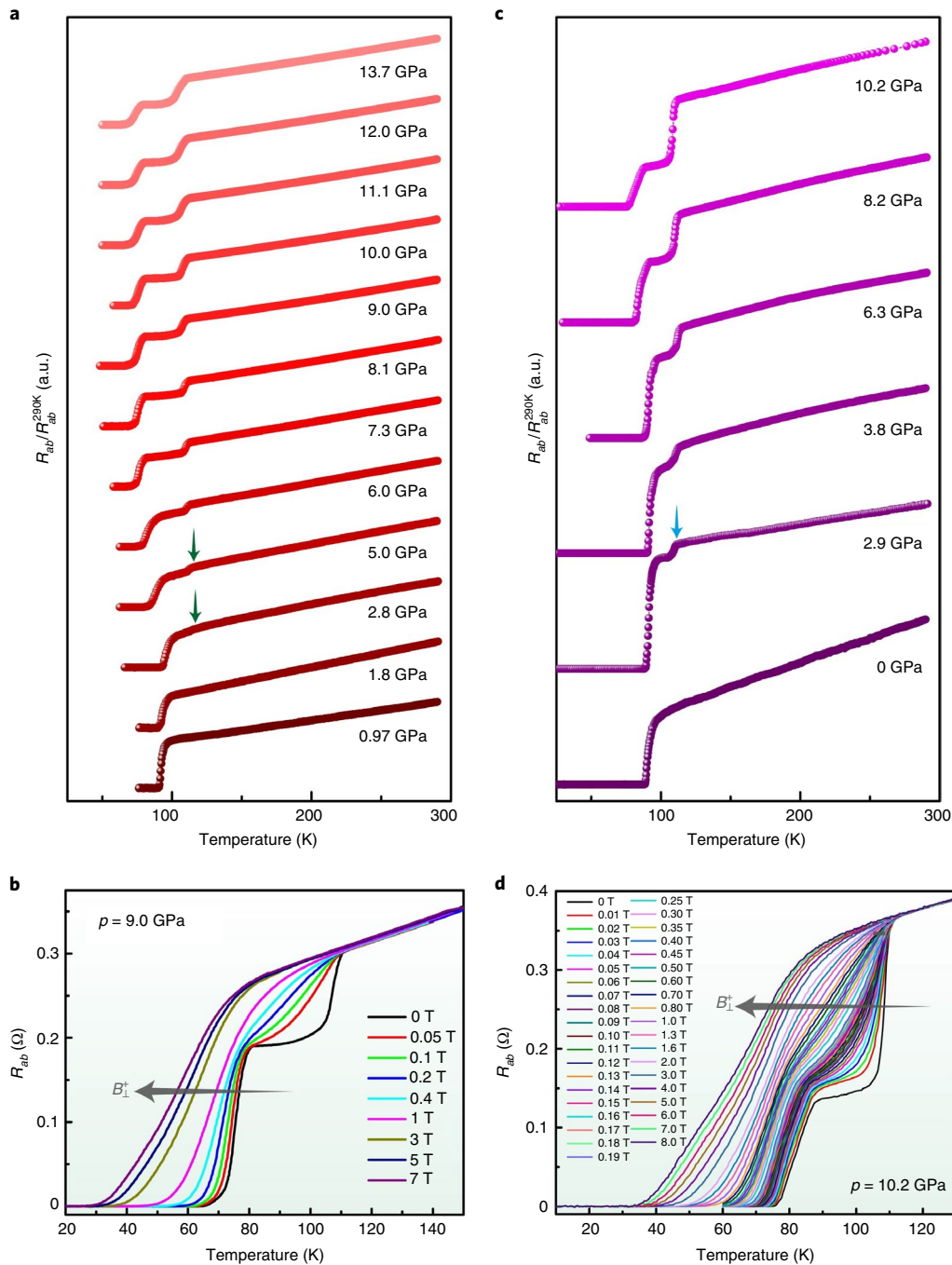


Fig. 1 | Characterization of the superconducting properties of optimally doped $\text{Bi}_2\text{Sr}_2\text{CaCu}_2\text{O}_{8+\delta}$ under pressure. a,c, Temperature dependence of in-plane electrical resistance at different pressures for two experimental runs. The arrows indicate the onset of the higher-temperature resistance drop discussed in the main text. **b,d,** Magnetic field dependence of superconducting transition temperatures measured on the sample subjected to 9.0 GPa (**b**) and 10.2 GPa (**d**).

resistance drop in $R_{ab}(T)$ also occurs at the same temperature. Therefore, the coincident resistance drops at 90 K signify the bulk (3D) superconducting transition in the sample. When we plotted the curves of $R_c(T)$ and $R_{ab}(T)$, obtained at the same pressure in the same figure, we found that the perturbation temperature in $R_c(T)$ is in excellent agreement with the temperature of the higher-temperature resistance drop in $R_{ab}(T)$ for each pressure point (Fig. 2a–d). Here, we define the higher-temperature T_C as T_C' and the lower-temperature T_C as T_C^{3D} .

To gain a more detailed understanding of this behaviour, we performed combined in situ high-pressure measurements of a.c.

susceptibility and resistance for the same sample in the same diamond anvil cell. This demanding combined measurement for studies of superconductivity under high pressure is full of technical challenges, because integration of the standard four probes for resistance measurements and the coils for a.c. susceptibility measurements into the same pressure cell is very difficult. Figure 2e–h presents plots of a.c. susceptibility ($\Delta\chi'$) versus temperature obtained at different pressures. The superconducting transition of the sample can be identified by the onset of deviation in the signal from the almost constant background on the high-temperature side (blue plots) and the rapid decrease to zero resistance (red plots).

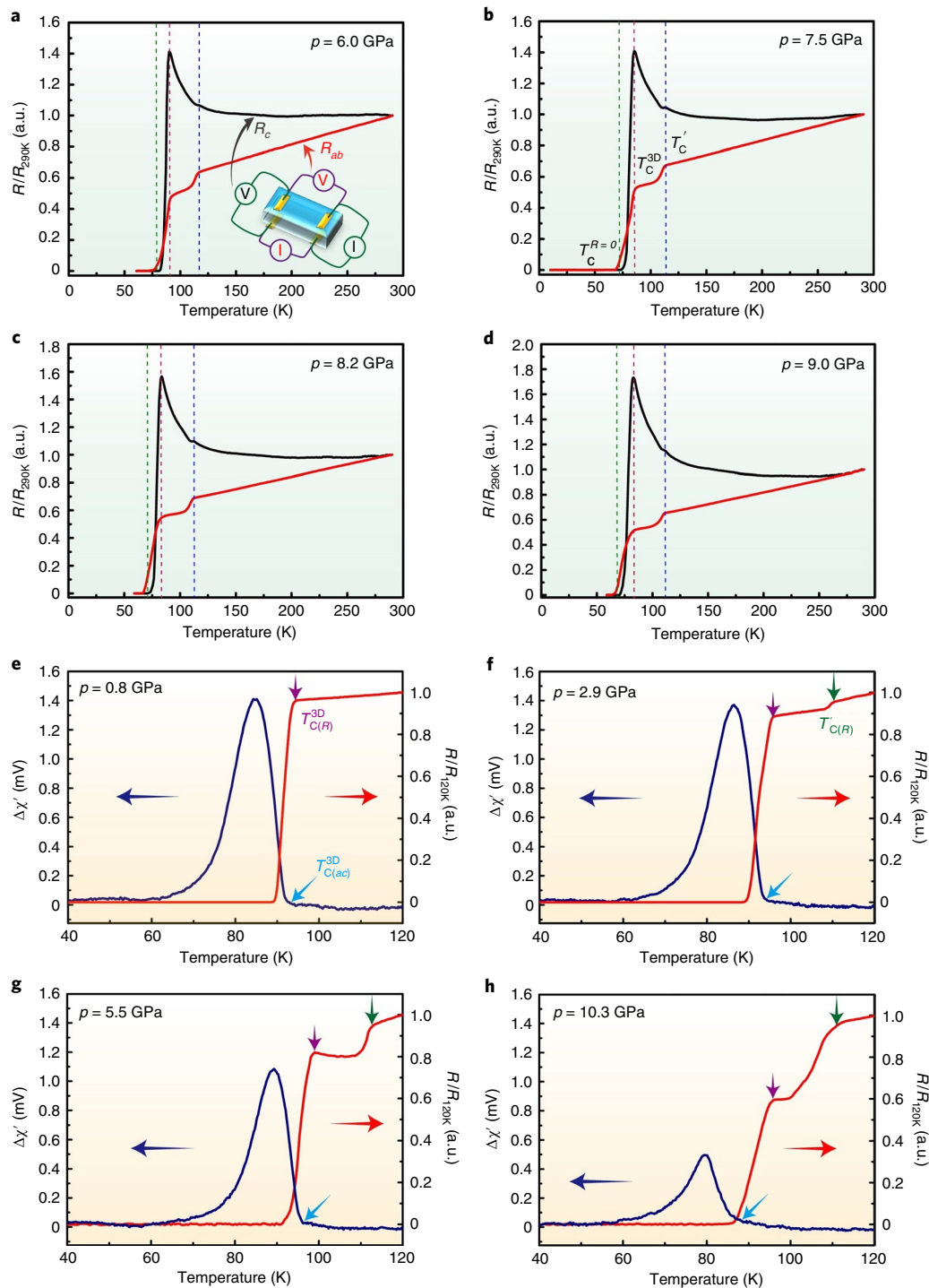


Fig. 2 | R_{ab} , R_c and $\Delta\chi'$ as a function of temperature for optimally doped $\text{BiSr}_2\text{CaCu}_2\text{O}_{8-\delta}$. **a-d**, $R_{ab}(T)$ and $R_c(T)$ measured at pressures of 6.0 (**a**), 7.5 (**b**), 8.2 (**c**) and 9.0 GPa (**d**). The inset in **a** shows the integration of electrodes for current measurements of $R_{ab}(T)$ and $R_c(T)$. $T_C^{R=0}$ (green dashed lines) and T_C^{3D} (red dashed lines) indicate the zero resistance and the onset of the 3D superconducting transition temperatures, and T_C' (blue dashed lines) represents the onset temperature of the higher-temperature superconducting state. **e-h**, $\Delta\chi'(T)$ and $R/R_{120\text{K}}$ at pressures of 0.8 (**e**), 2.9 (**f**), 5.5 (**g**) and 10.3 GPa (**h**). Purple and green arrows indicate T_C^{3D} and T_C' ; the cyan arrow indicates the T_C^{3D} probed by the a.c. susceptibility measurements.

At 0.8 GPa, the zero resistance and the diamagnetism of the ambient-pressure superconducting phase with a 3D nature are clearly visible. However, the diamagnetic signal of the higher-temperature superconducting state observed in $R_{ab}(T)$ is not captured by our a.c. susceptibility measurements within the pressure range we investigated. This indicates that the pressure-induced

higher-temperature superconducting state in the optimally doped Bi-2212 may have an unusual nature.

To understand the peculiar nature of the higher-temperature superconductivity, we applied the magnetic field perpendicular (B_{\perp}) and parallel (B_{\parallel}) to the a - b plane for the compressed sample at 10.1 GPa. As shown in Fig. 3a and Supplementary Figs. 2 and 3,

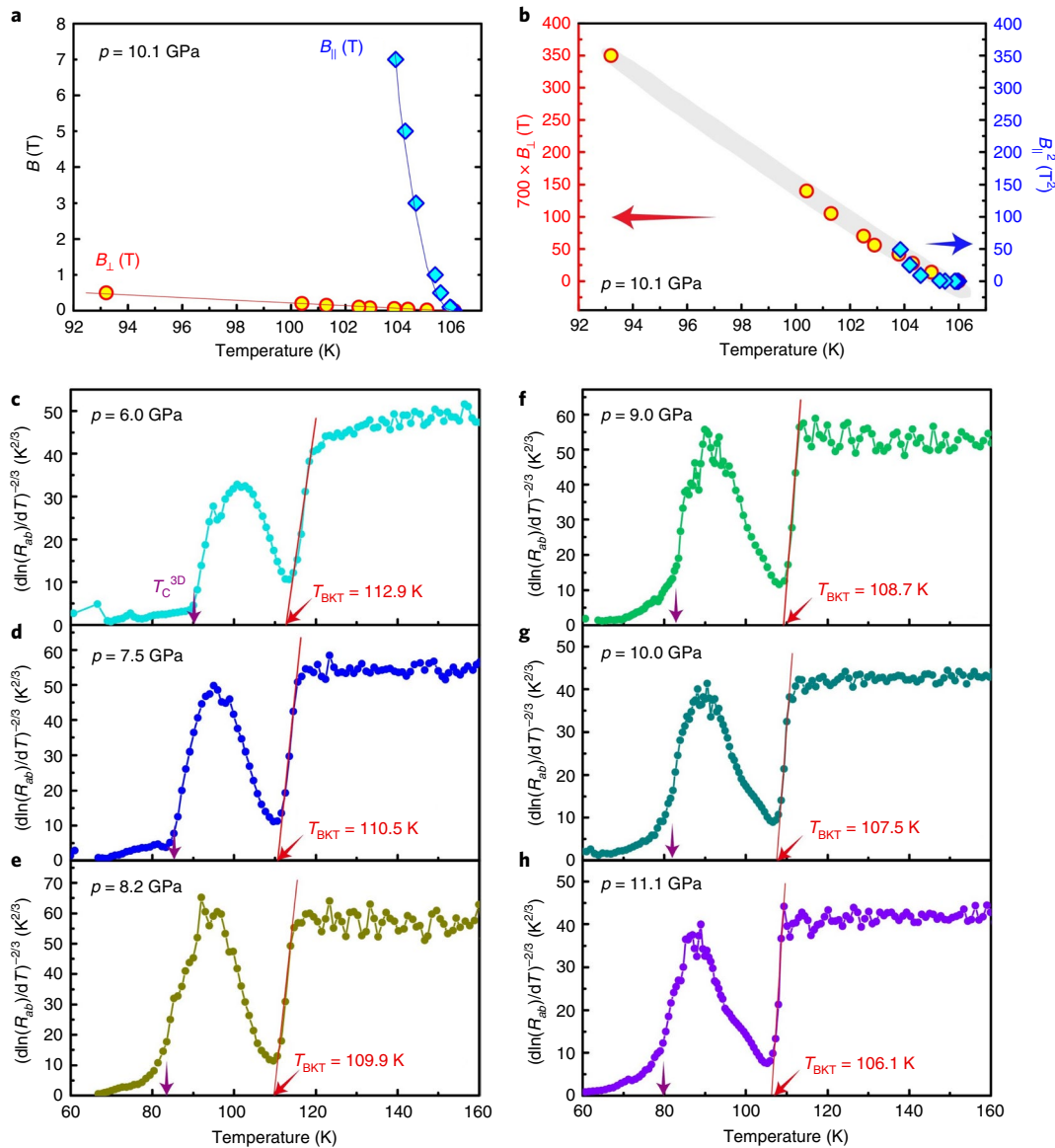


Fig. 3 | Analysis of the 2D superconducting properties of optimally doped $\text{Bi}_2\text{Sr}_2\text{CaCu}_2\text{O}_{8-\delta}$. **a**, Temperature dependence of magnetic fields B_{\perp} and B_{\parallel} . **b**, Scaling analysis for magnetic fields B_{\perp} and B_{\parallel} versus temperature (T), showing that B_{\parallel}^2 is ~ 700 times higher than B_{\perp} . The shaded area represents the scaling behaviour. **c–h**, Plots of $\text{dln}(R_{ab})/(\text{dT})^{-2/3}$ versus temperature, derived from the form of $R_{ab}(T) = R_0 \exp(-b(T/T_{\text{BKT}} - 1)^{-1/2})$, at different pressures. The red lines are fitting curves. The purple and red arrows indicate the temperatures of the 3D superconducting transition and the BKT-like transition, respectively.

the superconductivity shows strongly anisotropic characteristics, sustainable up to 7 T under the parallel magnetic field but suppressed above 0.5 T under the perpendicular magnetic field. We derived the scaling behaviour of B_{\perp} and B_{\parallel} as a function of temperature for the higher-temperature superconducting state and found distinct temperature dependences for $B_{\perp}(T)$ and $B_{\parallel}(T)$, namely $B_{\perp}(T) \propto (1 - T/T_C)$ versus $B_{\parallel}(T) \propto (1 - T/T_C)^{0.5}$ (Fig. 3b). The result of our scaling analysis leads to $B_{\parallel}^2(T) \approx 700 \times B_{\perp}(T)$, a typical feature for 2D superconductivity^{26,27}.

The remarkably anisotropic behaviour of the higher-temperature superconductivity is reminiscent of the Berezinskii–Kosterlitz–Thouless (BKT) transition at which vortex–antivortex pairs unbind¹⁰. It is known that the BKT transition in 2D superconductors is shown by the temperature (T) dependence of the resistance via $R_{ab}(T) = R_0 \exp(-b(T/T_{\text{BKT}} - 1)^{-1/2})$ (where R_0 and b are material parameters and T_{BKT} is the BKT transition temperature)²⁸. As illustrated in Fig. 3c–h, the results from our $R_{ab}(T)$ measurements at different

pressures are consistent with the BKT-like behaviour of the 2D film superconductors^{26,27}, also suggesting that the higher-temperature superconductivity is a 2D superconductivity.

We summarize our experimental results in the pressure– T_C phase diagram in Fig. 4. It is seen that the 2D superconducting state with a BKT-like behaviour emerges from the strange metal state above a critical pressure of 2.8 GPa, and then the T_C of the 2D superconducting state displays the same trend as that of the 3D superconducting state upon compression. The emergence of this 2D superconducting transition provides direct and strong evidence that the strange metal state is predominantly 2D-like²⁹.

In addition, our high-pressure powder X-ray diffraction measurements show that the sample holds its ambient-pressure structure up to the maximum pressure (14.4 GPa) of this study (Supplementary Fig. 4), implying that the crossover from 2D to 3D superconductivity is not related to the pressure-induced structural phase transition. Careful examination of the X-ray diffraction patterns shows that the

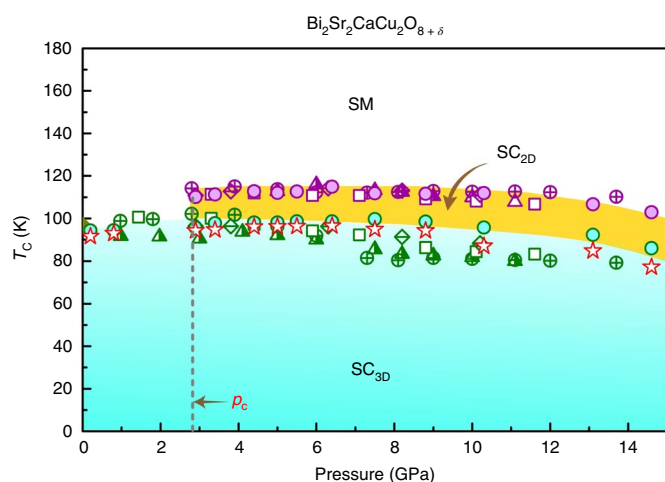


Fig. 4 | Pressure- T_c phase diagram of optimally doped $\text{Bi}_2\text{Sr}_2\text{CaCu}_2\text{O}_{8+\delta}$. $\text{SC}_{2\text{D}}$ and $\text{SC}_{3\text{D}}$ indicate the 2D (BKT-like) and 3D superconducting states, respectively, SM the strange metal state and p_c the critical pressure above which the 2D superconductivity emerges from the SM state.

intensity of the peak at $\sim 5^\circ$, associated with the diffraction of the (004) plane, increases upon compression (Supplementary Fig. 4). Usually, if a weak peak for the powdered sample of a 2D material becomes stronger under pressure without a structure phase transition, it is related to the pressure-induced reorientation of the polycrystalline sample³⁰. In the present study, it is likely that the (004) plane forms the preferred orientations of the lattice more easily due to its layered crystal structure. If so, this implies that the increment of the peak intensity has no correlation with the 2D superconducting state. However, given that the pressure-induced increment of the peak intensity appears at a pressure between 2.4 GPa and 3.9 GPa, just in the range (~ 3 GPa) of the emerging 2D superconducting state, it is natural to ask whether this increment of the peak intensity of the (004) plane is associated with the emergence of the 2D superconducting state. This may be a crucial question and deserves further experimental and theoretical investigations.

We also performed the same high-pressure resistance measurements on the underdoped and overdoped Bi-2212 samples. On looking in detail at $R_{ab}(T)$ of the underdoped sample, we found very weak kinks in the temperature range of the first resistance drop at pressures of 11.1 GPa and 15.0 GPa (Supplementary Fig. 5a), highlighting the possible existence of the two-transition behaviour in the underdoped sample. If true, the less obvious two-transition behaviour may be attributed to the existence of the pseudogap state, which may mask the resistance signal of the 2D superconducting state. In the overdoped sample, no evidence of the crossover from 2D to 3D superconducting state was observed (Supplementary Fig. 5b). These results suggest that the anomalous Fermi liquid state in the overdoped superconductor may prevent formation of the pressure-induced 2D superconducting state.

It is noteworthy that the pressure-induced crossover from 2D to 3D superconducting states found in this study has not been reported in any other compressed bulk cuprate superconductors, despite the fact that a similar magnetic field-induced crossover has been reported for $\text{La}_{2-x}(\text{Sr}/\text{Ba})_x\text{CuO}_4$ (ref. 31). This finding may thus aid in achieving a breakthrough in better understanding high- T_c superconductors. Consequently, we pose some questions stimulated by these results. First, is crossover associated with the interaction between the Jahn–Teller effect and the effect of high pressure? Next, why can such a crossover be observed in the optimally doped Bi-2212 superconductor via pressure and may exist in underdoped samples, but is not captured in overdoped superconductors? Finally,

can this pressure-induced phenomenon be observed in any other kind of hole-doped cuprate superconductor? These questions are of great interest for achieving a unified understanding of the cuprate superconductors and deserve further investigations, including sophisticated theoretical studies and challenging high-pressure measurements with the capacity for detecting dynamic physics.

Online content

Any methods, additional references, Nature Research reporting summaries, source data, extended data, supplementary information, acknowledgements, peer review information; details of author contributions and competing interests; and statements of data and code availability are available at <https://doi.org/10.1038/s41567-019-0740-0>.

Received: 14 July 2019; Accepted: 5 November 2019;

Published online: 16 December 2019

References

- Keimer, B., Kivelson, S. A., Norman, M. R., Uchida, S. & Zaanen, J. From quantum matter to high-temperature superconductivity in copper oxides. *Nature* **518**, 179–186 (2015).
- Zaanen, J. Superconducting electrons go missing. *Nature* **536**, 282–283 (2016).
- Norman, M. R. & Pépin, C. The electronic nature of high temperature cuprate superconductors. *Rep. Prog. Phys.* **66**, 1547–1610 (2003).
- Coleman, P. & Schofield, A. J. Quantum criticality. *Nature* **433**, 226–229 (2005).
- Vishik, I. M. Photoemission perspective on pseudogap, superconducting fluctuations and charge order in cuprates: a review of recent progress. *Rep. Prog. Phys.* **81**, 062501 (2018).
- Ding, H. et al. Spectroscopic evidence for a pseudogap in the normal state of underdoped high- T_c superconductors. *Nature* **382**, 51–54 (1996).
- Zaanen, J. Planckian dissipation, minimal viscosity and the transport in cuprate strange metals. *SciPost Phys.* **6**, 061 (2019).
- Greene, R. L., Mandal, P. R., Poniatowski, N. R. & Sarkar, T. The strange metal state of the electron-doped cuprates. Preprint at <https://arxiv.org/abs/1905.04998> (2019).
- Bozovic, I., He, X., Wu, J. & Bollinger, A. T. Dependence of the critical temperature in overdoped copper oxides on superfluid density. *Nature* **536**, 309–311 (2016).
- Beasley, M. R., Mooij, J. E. & Orlando, T. P. Possibility of vortex–antivortex pair dissociation in two-dimensional superconductors. *Phys. Rev. Lett.* **42**, 1165–1168 (1979).
- Bednorz, J. G. & Müller, K. A. Possible high T_c superconductivity in the Ba–La–Cu–O system. *Z. Phys. B* **64**, 189–193 (1986).
- Wu, M. K. et al. Superconductivity at 93 K in a new mixed-phase Y–Ba–Cu–O compound system at ambient pressure. *Phys. Rev. Lett.* **58**, 908–910 (1987).
- Chu, C. W., Deng, L. Z. & Lv, B. Hole-doped cuprate high temperature superconductors. *Physica C* **514**, 290–313 (2015).
- Proust, C. & Taillefer, L. The remarkable underlying ground states of cuprate superconductors. *Annu. Rev. Condens. Matter Phys.* **10**, 409–429 (2019).
- Anderson, P. W. The resonating valence bond state in La_2CuO_4 and superconductivity. *Science* **235**, 1196–1198 (1987).
- Varma, C. M., Littlewood, P. B., Schmitt-Rink, S., Abrahams, E. & Ruckenstein, A. E. Phenomenology of the normal state of Cu–O high-temperature superconductors. *Phys. Rev. Lett.* **63**, 1996–1999 (1989).
- Dagotto, E. Correlated electrons in high-temperature superconductors. *Rev. Mod. Phys.* **66**, 763–840 (1994).
- Su, Y. H., Luo, H. G. & Xiang, T. Universal scaling behavior of the c -axis resistivity of high-temperature superconductors. *Phys. Rev. B* **73**, 134510 (2006).
- Dai, Z. H., Zhang, Y. H., Senthil, T. & Lee, P. A. Pair-density waves, charge-density waves and vortices in high- T_c cuprates. *Phys. Rev. B* **97**, 174511 (2018).
- Celebrating 125 years of *The Physical Review*. <https://journals.aps.org/125years> (American Physical Society, 2018).
- Meng, J. Q. et al. Coexistence of Fermi arcs and Fermi pockets in a high- T_c copper oxide superconductor. *Nature* **462**, 335–338 (2009).
- Chen, X. J. et al. Enhancement of superconductivity by pressure-driven competition in electronic order. *Nature* **466**, 950–953 (2010).
- Drozdov, I. K. et al. Phase diagram of $\text{Bi}_2\text{Sr}_2\text{CaCu}_2\text{O}_{8+\delta}$ revisited. *Nat. Commun.* **9**, 5210 (2018).
- Ruan, W. et al. Visualization of the periodic modulation of Cooper pairing in a cuprate superconductor. *Nat. Phys.* **14**, 1178–1182 (2018).

25. Deng, L. Z. et al. Higher superconducting transition temperature by breaking the universal pressure relation. *Proc. Natl Acad. Sci. USA* **116**, 2004–2008 (2019).
26. Zhang, H. M. et al. Detection of a superconducting phase in a two-atom layer of hexagonal Ga film grown on semiconducting GaN (0001). *Phys. Rev. Lett.* **114**, 107003 (2015).
27. Reyren, N. et al. Superconducting interfaces between insulating oxides. *Science* **317**, 1196–1199 (2007).
28. Satto, Y., Nojima, T. & Iwasa, Y. Highly crystalline 2D superconductors. *Nat. Rev. Mater.* **2**, 16094 (2017).
29. Boeinger, G. S. An abnormal normal state. *Science* **323**, 590–591 (2009).
30. Mao, W. et al. Bonding changes in compressed superhard graphite. *Science* **302**, 425–427 (2003).
31. Li, Q., Hücker, M., Gu, G. D., Tsvelik, A. M. & Tranquada, J. M. Two-dimensional superconducting fluctuations in stripe-ordered $\text{La}_{1.875}\text{Ba}_{0.125}\text{CuO}_4$. *Phys. Rev. Lett.* **99**, 067001 (2007).

Publisher's note Springer Nature remains neutral with regard to jurisdictional claims in published maps and institutional affiliations.

© The Author(s), under exclusive licence to Springer Nature Limited 2019

Methods

As-grown optimally doped single-crystal rods of $\text{Bi}_x\text{Sr}_y\text{CaCu}_2\text{O}_{8+\delta}$ were grown by the floating zone method as described in ref.³². Before the experiments, the crystals were cleaved to expose fresh surfaces.

High pressure was generated with a diamond anvil cell made of BeCu alloy (with a 300 μm culet) in different independent measurements. A four-probe method was used for the resistance, and magnetoresistance measurements. A mixture of Al_2O_3 powder and epoxy was adopted as an insulating layer. To provide the sample in a quasi-hydrostatic pressure environment, NaCl powder was employed as the pressure transmitting medium.

High-pressure magnetic susceptibility measurements were carried out in a diamond anvil cell (fabricated from CuBe alloy) with a gas membrane system. To minimize the temperature-dependent background, a gasket made from non-magnetic NiCr alloy was adopted. The sample was surrounded by a secondary coil (pickup coil) and a field-generating primary coil wound on top of the secondary coil. The alternating flux through the pickup coil produced an a.c. voltage, which was the measured signal. When the sample was cooled below T_c , the field was expelled from the sample due to the superconducting shielding effect, forcing some of the flux lines out of the pickup coil and leading to a reduction in the induced voltage in the pickup coil^{33–35}. To increase the measurement accuracy for the small sample, we used two phase-locked amplifiers to collect the diamagnetic signal: the real part of the a.c. susceptibility (χ'^{-1}) stimulated by the current source at 13.83 kHz was collected by the first lock-in amplifier and another real part of the a.c. susceptibility (χ'^{-2}) stimulated by the current source at 13.3 Hz was collected by the second lock-in amplifier. Here, $\Delta\chi'(B) = \chi'^{-1}(B_1) - \chi'^{-2}(B_2)$ ($B_1 = 9.9$ mT and $B_2 = 0$ T). Therefore, the a.c. susceptibility measured here was modulated by the magnetic field oscillating at 13.3 Hz, which was resolved by the second lock-in amplifier at the second harmonic from the output of the first lock-in amplifier. Such a magnetic field-modulated $\chi'(B)$ has been used by the Geophysics laboratory in the Carnegie Institute for studies of the pressure effect on superconductivity and pressure-induced superconductivity^{23,36}. Consequently, the results of $\chi'(B)$ have a peak-like function instead of a step-like function, which was collected by a single phase-locked amplifier.

High-pressure powder X-ray diffraction measurements were carried out at beamline 15U at the Shanghai Synchrotron Radiation Facility. A monochromatic X-ray beam with a wavelength of 0.6199 Å was used for measurements. Silicone oil served as the pressure-transmitting medium.

Pressure in all measurements was determined by the ruby fluorescence method³⁷.

Data availability

The data represented in Figs. 1–4 are available with the online version of this paper. All other data that support the findings of this study are available from the corresponding authors on request.

References

- Gu, G. D., Takamuku, K., Koshizuka, N. & Tanaka, S. Large single crystal Bi-2212 along the *c*-axis prepared by floating zone method. *J. Cryst. Growth* **130**, 325–329 (1993).
- Timofeev, Y. A., Struzhkin, V. V., Hemley, R. J., Mao, H.-K. & Gregoryanz, E. A. Improved techniques for measurement of superconductivity in diamond anvil cell by magnetic susceptibility. *Rev. Sci. Instrum.* **73**, 371–377 (2002).
- Hamlin, J. J., Tissen, V. G. & Schilling, J. S. Superconductivity at 17 K in yttrium metal under nearly hydrostatic pressures up to 89 GPa. *Phys. Rev. B* **73**, 094522 (2006).
- Sun, L. L. et al. Re-emerging superconductivity at 48 kelvin in iron chalcogenides. *Nature* **483**, 67–69 (2012).
- Struzhkin, V. V., Hemley, R. J., Mao, H. K. & Timofeev, Y. A. Superconductivity at 10–17 K in compressed sulphur. *Nature* **390**, 382–384 (1997).
- Mao, H. K., Xu, J. & Bell, P. M. Calibration of the ruby pressure gauge to 800 kbar under quasi-hydrostatic conditions. *J. Geophys. Res.* **91**, 4673–4676 (1986).

Acknowledgements

We thank Q.-K. Xue, X.-C. Ma, J. Wang, D.-H. Lee, H. Yao and Z. Weng for helpful discussions. This work in China was supported by the National Key Research and Development Program of China (grants 2017YFA0302900, 2016YFA0300300 and 2017YFA0303103), the NSF of China (grants 11427805, U1532267 and 11604376) and the Strategic Priority Research Program (B) of the Chinese Academy of Sciences (CAS, grant XDB25000000). J.G. is grateful for support from the Youth Innovation Promotion Association of CAS (2019008). The work at Brookhaven National Laboratory was supported by the Office of Basic Energy Sciences, Division of Materials Sciences and Engineering, US Department of Energy, under contract no. DE-SC0012704.

Author contributions

L.S., T.X. and Q.W. designed the research. J.G., Y.Z., C.H., Y.S. and L.S. performed high-pressure resistance, magnetoresistance and a.c. susceptibility measurements. G.G. grew the single crystals. J.G., S.C., C.Y., G.L., K.Y. and A.L. carried out high-pressure X-ray diffraction measurements. L.S., Q.W., T.X., J.G. and Y.Z. wrote the paper. All authors analysed the data and discussed the results.

Competing interests

The authors declare no competing interests.

Additional information

Supplementary information is available for this paper at <https://doi.org/10.1038/s41567-019-0740-0>.

Correspondence and requests for materials should be addressed to L.S.

Peer review information *Nature Physics* thanks Derrick VanGennep, Maw-Kuen Wu and the other, anonymous, reviewer(s) for their contribution to the peer review of this work.

Reprints and permissions information is available at www.nature.com/reprints.